IEEE Access
Multidisciplinary | Rapid Review | Open Access Journal

Received October 30, 2019, accepted December 11, 2019, date of publication December 18, 2019,
date of current version December 31, 2019.

Digital Object Identifier 10.1109/ACCESS.2019.2960607

Adaptive Finite-Time PI Sliding Mode Trajectory Tracking Control for Underactuated Hovercraft With Drift Angle Constraint

MINGYU FU, TAN ZHANG, AND FUGUANG DING
College of Automation, Harbin Engineering University, Harbin 150001, China

Corresponding author: Fuguang Ding (dingfuguang@hrbeu.edu.cn)

This work was supported in part by the National Natural Science Foundation of China under Grant 51309062 and in part by the Project Research on Maneuverability of High Speed Hovercraft under Project 2007DFR80302.

ABSTRACT Considering the sailing characteristics and difficult maneuverability of hovercraft, the three degree-of-freedom (DOF) mathematical model cannot describe effectively the motion of hovercraft. Therefore, a mathematical model of four-DOF motion of hovercraft is established. This paper addresses the trajectory tracking problem of the hovercraft with finite-time convergence to equilibrium point, model uncertainty, external disturbance and drift angle constraint based on the four-DOF model. A novel robust tracking controller is proposed by combining finite-time observer with adaptive sliding mode control to solve the problem of the finite-time convergence and handle approximation error. In order to ensure the safe navigation of the hovercraft, a safety constraint auxiliary system is designed to restrain the drift angle in real time. Furthermore, a finite-time observer is designed to estimate and compensate model uncertainties and external disturbances. We show that under the proposed control scheme, all tracking errors can converge to zero in finite time, the drift angle can be constrained in real time and all closed-loop signals are guaranteed to be bounded. Finally, the numerical simulation results show the effectiveness of the proposed method.

INDEX TERMS PI sliding mode control, finite-time observer, finite-time control, model uncertainties, state constraint.

I. INTRODUCTION

There is flexible skirt around the bottom of underactuated hovercraft for sealing the cushion air. By constantly pressing high pressure air of the cushion lift fan into the flexible skirt, the hovercraft can get sufficient cushion lift force for sailing to obtain its unique amphibious property [1]. It can sail at high speed over shoals, sandy beaches, marshes, ice and other environments, where no other surface vessels can arrive [1]. In recent decades, due to its unique performance, hovercraft has attracted more and more attention in Marine research, such as Marine resources exploration, rescue, transportation, military missions and other fields.

It is worth noting that the hovercraft has very little contact with the water and low righting moments result in turning rudder is to easily produce a large roll angle and stern-kickoff, so that it runs in a dangerous situation. The lateral component of the force of air cushion force under large roll angle makes the ship drift sideways and loses course stability, which may cause the ship capsizing accident. At the same time, the hovercraft has very weak anti-interference ability and poor navigation stability, which may cause the capsizing accident when it is disturbed by the external environment or when the pilots turn the rudder in the emergency state. Or the skirt of the hovercraft's bow touches the water, resulting in a negative pitch angle, and then the bow appears to plough-in, a large yaw angle, drift angle, and large roll angle until the ship capsize [2]–[4]. Considering that the above dangerous navigation situation is closely related to the roll angle of hovercraft, this paper establishes a four- DOF motion mathematical model of hovercraft by taking roll degree of freedom into account, which is closer to the motion characteristics of real ship than the three- DOF model.

Usually the main actuators of the hovercraft include two air propellers at the stern and a vertical air rudder mounted behind every propeller. The propellers mainly provide the forward power and the rudders provide the turning moment. Therefore, hovercraft is a kind of typical underactuated ship.

The associate editor coordinating the review of this manuscript and approving it for publication was Zhiguang Feng.

The main difficulty for underactuated surface ship control is that the lateral axis is not directly actuated and the number of independent actuators in the underactuated system is less than the number of degrees of freedom. The challenge to control underactuated surface vessels is how to use two independent actuators to control the ship's four-DOF motion in the presence of model uncertainty and external disturbances. In the past 20 years, in order to overcome the above difficulties, various underactuated surface ship control methods have been proposed through the efforts of researchers, and great achievements have been achieved. Due to the parameter uncertainty and high nonlinearity of underactuated surface ships, some so-called robust control algorithms have been proposed, such as sliding mode control [5]–[9], neural network control [10]–[12], robust adaptive control [13]–[15], H_∞ robust control [16], backstepping techniques [17]–[20], fuzzy control [21]–[23], [30]. In ship motion control, the above methods are very effective in dealing with environmental disturbance and model uncertainty.

Recently, considering the robustness of ship control, literature [24] adopted the biological inspired method for trajectory tracking control of underactuated surface ships, and used the single-layer neural network to approximate the unknown dynamics including uncertain model parameters and hydrodynamic coefficients, thus solving the problem of model uncertainty. In [25], a practical adaptive neural network tracking controller is proposed by using backstepping technique and neural network minimum parameter learning method in the case of imprecise model information and external disturbance. A unified online adaptive nearly optimal control framework for linear and nonlinear systems with parametric uncertainties is presented in [26]. Under this framework, an auxiliary system which converges to the unknown dynamics is constructed to approximate and compensate the parameter uncertainty. An adaptive dynamic sliding mode control method for trajectory tracking control of under-actuated underwater unmanned vehicle is proposed in [6], but the proposed adaptive sliding mode control requires some assumptions, such as the existence of first derivative of external disturbance and control input. In [27], an adaptive fuzzy H_∞ control method is proposed for the problem of ship steering to keep the influence of model error and external disturbance on tracking error below any ideal level. In [29] used the combination of neural network and terminal sliding mode to design a finite time trajectory tracking controller for underactuated hovercraft, but the designed sliding mode surface is asymptotically convergent. Considering ship dynamic positioning system with the unknown model parameters and unknown time varying environment disturbance, an adaptive fuzzy controller is proposed in [21], the adaptive fuzzy system combined with vector backstepping method is utilized to estimate the unknown dynamics model parameters and unknown time varying environmental disturbance. In [22], an adaptive fuzzy stabilization controller is designed for underactuated surface ships in the presence of unknown time-varying environmental disturbances. The adaptive fuzzy system is used to approximate the uncertain terms caused by unknown time-varying environmental disturbances in the control law. The finite time PI sliding mode control of hypersonic vehicles is proposed in [37], however, the structure of the designed controller is not conductive to the combination with other control strategies.

Motivated by the above-mentioned observations, a novel finite-time adaptive PI sliding mode trajectory tracking control strategy for underactuated hovercraft with drift Angle constraint is proposed. In particular, in comparison with the controllers to ensure asymptotic convergence in [29], the sliding mode manifold in this paper can converge to zero in finite time. The special structure of the designed PI sliding mode control strategy can relax some assumptions in [6], [29], such as the existence of the first derivative of the control input. Considering the safe navigation of hovercraft, the drift angle constraint auxiliary system is designed to constrain the drift angle in real time, so as to ensure the safe navigation of hovercraft. The tracking error of the control system can converge to zero in finite time and all signals in the closed loop system are bounded. Finally, the effectiveness and robustness of the proposed controller are verified by numerical simulations.

The rest of the paper is arranged as follows: The preliminaries and problem formulation are given and the four-DOF motion model of underactuated hovercraft with model uncertainty and external disturbance is established in Section 2. Section 3 is devoted to the finite time adaptive PI sliding mode trajectory tracking controllers design for the hovercraft with drift angle constraint under model uncertainty and external disturbance. Numerical simulation results are showed in Section 4. Section 5 concludes the work of this paper.

II. PRELIMINARIES AND PROBLEM FORMULATION

A. PRELIMINARIES

Lemma 1 [31]: Considering a n-th order system as follows:

$$\begin{aligned} \dot{x}_1 &= x_2 \\ \dot{x}_2 &= x_3 \\ &\cdots \\ \dot{x}_n &= u \end{aligned} \tag{1}$$

if the controller we developed ensures that the following equation is true:

$$\dot{x}_n + k_n sign\,(x_n)\,|x_n|^{\alpha_n} + \cdots + k_1 sign\,(x_1)\,|x_1|^{\alpha_1} = 0 \tag{2}$$

the states $[x_1, \cdots, x_n]^T$ of the system can converge to the equilibrium point in finite time t_f. Where k_i and $\alpha_i\,(i = 1, 2, \ldots, n)$ are positive constant. k_i can be selected such that the polynomial $p^n + k_n p^{n-1} + \cdots + k_2 p^2 + k_1$ is Hurwitz, i.e., the eigenvalues of the polynomial are all in the left-half side of the complex plane. α_i can be selected based on the following equation:

$$\begin{cases} \alpha_1 = \alpha, \quad n = 1 \\ \alpha_{i-1} = \dfrac{\alpha_i \alpha_{i+1}}{2\alpha_{i+1} - \alpha_i}, \quad i = 2, \ldots, n \quad \forall n \geq 2 \end{cases} \tag{3}$$

where $\alpha_{n+1} = 1, \alpha_n = \alpha, \alpha \in (1 - \varepsilon, 1)\,, \varepsilon \in (0, 1)$.

Lemma 2 [32], [33]: A second-order system with perturbation has the following form:

$$\begin{cases} \dot{x}_1 = -k_1 |x_1|^{1/2} sign(x_1) + x_2 \\ \dot{x}_2 = -k_2 sign(x_1) + \rho(x_1, x_2, t) \end{cases} \tag{4}$$

where x_1 and x_2 are the state variable, k_1 and k_2 are the design gain, $\rho(x_1, x_2, t)$ is the perturbation term, and there is a constant $L > 0$, such that $|\rho(x_1, x_2, t)| \leq L$ is true. For any constant L and the existence of gain k_1 and k_2 makes the system (4) stable globally the equilibrium point $x_1 = 0$ and $x_2 = 0$ in finite time.

Lemma 3 [34]: For any real numbers $x_1, \ldots x_n$ and $0 < b < 1$, then the following inequality holds:

$$(|x_1| + \cdots + |x_n|)^b \leq |x_1|^b + \cdots + |x_n|^b \tag{5}$$

Lemma 4 [35]: For any real numbers $\lambda_1 > 0$, $\lambda_2 > 0$, $0 < l < 1$, if an extended Lyapunov condition function $V(x)$ satisfies inequality $\dot{V}(x) + \lambda_1 V(x) + \lambda_2 V^l(x) \leq 0$, then $V(x)$ is finite-time convergent. The convergence time that $V(x)$ converges to zero from initial moment t_0 can be determined by

$$t_s \leq t_0 + \frac{1}{\lambda_1 (1-l)} \ln \frac{\lambda_1 V^{1-l}(x(t_0)) + \lambda_2}{\lambda_2} \tag{6}$$

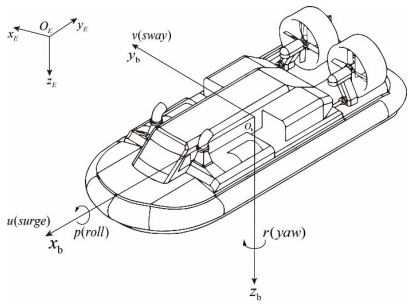

FIGURE 1. Reference frames of the hovercraft.

B. DYNAMIC MODEL OF A HOVERCRAFT

Based on the [29], the kinematic model and dynamic model are used to describe the four-DOF motion of the hovercraft in Fig.1, as follows:

$$\begin{cases} \dot{x} = u\cos\psi - v\sin\psi\cos\phi \\ \dot{y} = u\sin\psi + v\cos\psi\cos\phi \\ \dot{\phi} = p \\ \dot{\psi} = r\cos\phi \end{cases} \tag{7}$$

$$\begin{cases} \dot{u} = vr + \dfrac{F_{xD0}}{m_0} + f_u + \dfrac{\tau_u}{m_0} \\ \dot{v} = -ur + \dfrac{F_{yD0}}{m_0} + f_v \\ \dot{p} = \dfrac{M_{xD0}}{J_{x0}} + f_p \\ \dot{r} = \dfrac{M_{zD0}}{J_{z0}} + f_r + \dfrac{\tau_r}{J_{z0}} \end{cases} \tag{8}$$

with

$$\begin{aligned} f_u &= \frac{1}{m_0}(-\Delta m\dot{u} + \Delta mvr + \Delta F_{xD}) + \frac{d_u(t)}{m_0} \\ f_v &= -\frac{1}{m_0}\left(\Delta m(\dot{v} + ur) + \Delta F_{yD}\right) + \frac{d_v(t)}{m_0} \\ f_p &= \frac{1}{J_{x0}}(-\Delta J_x\dot{p} + \Delta M_{xD}) + \frac{d_p(t)}{J_{x0}} \\ f_r &= \frac{1}{J_{z0}}(-\Delta J_z\dot{r} + \Delta M_{zD}) + \frac{d_r(t)}{J_{z0}} \end{aligned} \tag{9}$$

where u, v, p and r represent the surge velocity, sway velocity, roll angular velocity and yaw angular velocity of the hovercraft in the body-fixed frame, respectively. x, y, ϕ and ψ denote position, roll angle and yaw angle of the hovercraft with respect to earth-fixed frame. The control inputs are surge force τ_u and yaw moment τ_r. m_0, J_{x0} and J_{z0} denote the known hull design mass and moment of inertia. Δm, ΔJ_x and ΔJ_z are considered uncertainty of hull mass and moment of inertia. F_{xD0}, F_{yD0}, M_{xD0} and M_{zD0} represent the part of the approximate model that can be calculated through certain test methods in the current resistance models of hovercraft such as air resistance, air momentum force, skirt resistance and wave-making resistance, etc. ΔF_{xD}, ΔF_{yD}, ΔM_{xD} and ΔM_{zD} denote the uncertainty of model parameters in water and air resistance and the model uncertainty caused by modeling errors. $d_u(t)$, $d_v(t)$, $d_p(t)$ and $d_r(t)$ represent disturbances, which are unmodeled hydrodynamic disturbances and affect the control accuracy. f_u, f_v, f_p and f_r represent the sum of model uncertainties and external disturbances. F_{xD0}, F_{yD0}, M_{xD0} and M_{zD0} can be determined by following equations:

$$\begin{aligned} F_{xa} &= -0.5\rho_a V_a^2 C_{xa} S_{PP} \\ F_{ya} &= -0.5\rho_a V_a^2 C_{ya} S_{LP} \\ M_{xa} &= -0.5\rho_a V_a^2 C_{mxa} S_{PP} l_c + F_{ya} z_a \\ M_{za} &= -0.5\rho_a V_a^2 C_{mza} S_{HP} H_{hov} + F_{ya} x_a + F_{xa} y_a \\ F_m &= \rho_a V_a Q \\ F_{wm} &= C_{wm} p_c^2 B_c \Big/ \rho_w g \\ F_{sk} &= 0.5 V_a^2 C_{sk} \left(h/l_{sk}\right)^{-0.34} l_{sk} S_c^{0.5} \\ &\quad + \left(2.8167\left(p_c/l_c\right)^{-0.259} - 1\right) F_{wm} \\ F_c &= 2l_c \varphi p_c \left(0.5 B_c \tan\phi + h_0\right) \\ M_G &= G h_m \tan\phi \\ F_{xD0} &= F_{xa} + F_m\cos\beta + F_{wm}\cos\beta + F_{sk}\cos\beta \\ F_{yD0} &= F_{ya} + F_m\sin\beta + F_{wm}\sin\beta + F_{sk}\sin\beta + F_c \\ M_{xD0} &= M_{xa} + F_m z_m \sin\beta + F_{wm} z_{wm}\sin\beta \\ &\quad + G h_m \tan\phi + F_{sk} z_{sk}\sin\beta + F_c z_c \\ M_{zD0} &= M_{za} + F_m x_m \sin\beta + F_m y_m \cos\beta \\ &\quad + F_{wm} x_{wm}\sin\beta + F_{wm} y_{wm}\cos\beta \\ &\quad + F_{sk} x_{sk}\sin\beta + F_{sk} y_{sk}\cos\beta + F_c x_c \end{aligned} \tag{10}$$

where F_{xa}, F_{ya}, M_{xa} and M_{za} are air resistances, F_m, F_{wm}, F_{sk} and F_c are air momentum force, wave-making resistance, skirt resistance and cushion resistance, respectively. C_{xa}, C_{ya},

C_{mxa}, C_{mza}, C_{wm} and C_{sk} are the corresponding resistance coefficients. M_G is roll restoring moment. l_c and B_c is the length and width of the cushion, respectively. S_{PP}, S_{LP} and S_{HP} are positive, lateral and horizontal projections. S_c is the cushion area, p_c means the cushion pressure, h means the average clearance for air leakage in static hovering mode, h_m and h_0 are metacentric height and initial lifting height, respectively. l_{sk} is the total length of the skirt, φ means flow coefficient, H_{hov} is the height of the hovercraft, ρ_a and ρ_w are air density and water density, respectively. z_a, z_m, z_{wm}, z_{sk} and z_c represent heights of each force's acting point relative to ship's mass center, (x_a, y_a), (x_m, y_m), (x_{wm}, y_{wm}), (x_{sk}, y_{sk}) and (x_c, y_c) represent the coordinates of these action points. β and V_a mean drift angle and relative wind speed, respectively. β and V_a can be determined by following equations:

$$\begin{aligned} \beta &= arctan\,(v/u) \\ V_a &= \sqrt{(u + V_\omega \cos(\beta_\omega - \psi))^2 + (v + V_\omega \sin(\beta_\omega - \psi))^2} \\ \beta_a &= arctan\left[\frac{v + V_\omega \sin(\beta_\omega - \psi)}{u + V_\omega \cos(\beta_\omega - \psi)}\right] \end{aligned} \tag{11}$$

where β_a represents relative wind direction, V_ω and β_ω mean absolute wind speed and direction, respectively.

Assumption 1: The motion of pitch and heave of hovercraft are ignored. The pressure of each air chamber and the flow of cushion fan are constant.

Assumption 2: The hovercraft is fitted with two same air propellers and two same air rudders, which are symmetrically mounted at the tail of the hovercraft. And the air rudder provides the turning moment, the propeller only provides the forward thrust.

Assumption 3: The model uncertainties f_u, f_v, f_p and f_r and their first time derivatives are bounded, that is $|f_i| \le T_{i\max}$, $|\dot{f}_i| \le T_{id\max}$ $(i = u, v, p, r)$, $T_{i\max}$ and $T_{id\max}$ are positive constants.

Remark 1: Since the uncertain terms f_u, f_v, f_p and f_r are functions of the system state variables and the unmodeled hydrodynamic disturbances, thus they are bounded, differentiable and their derivatives are bounded from [29]. Therefore, Assumption 3 is realistic in practice.

Assumption 4: The surge velocity u, sway velocity v and yaw angular velocity r of the hovercraft are bounded.

Remark 2: In the motion process of underactuated hovercraft, the surge velocity, sway velocity and yaw angular velocity of the hovercraft cannot be infinite due to the constraints of hydrodynamic damping term, air resistance and the ability of the actuator [36].

C. PROBLEM FORMULATION

For the convenience of description, we first define the desired reference trajectory in this paper. The target tracked by the hovercraft is generated by the virtual ship:

$$\begin{bmatrix} \dot{x}_d \\ \dot{y}_d \\ \dot{\psi}_d \end{bmatrix} = \begin{bmatrix} \cos\psi_d & -\sin\psi_d & 0 \\ \sin\psi_d & \cos\psi_d & 0 \\ 0 & 0 & 1 \end{bmatrix} \begin{bmatrix} u_{dset} \\ v_{dset} \\ r_{dset} \end{bmatrix} \tag{12}$$

Assumption 5: The tracking target states x_d,y_d,ψ_d and their first time derivatives are bounded.

We define the following position tracking errors:

$$\begin{bmatrix} x_e \\ y_e \end{bmatrix} = \begin{bmatrix} x \\ y \end{bmatrix} - \begin{bmatrix} x_d \\ y_d \end{bmatrix} \tag{13}$$

Using (7) and (13), the derivatives of the position errors are obtained as follows:

$$\begin{bmatrix} \dot{x}_e \\ \dot{y}_e \end{bmatrix} = \begin{bmatrix} \cos\psi & -\sin\psi\cos\phi \\ \sin\psi & \cos\psi\cos\phi \end{bmatrix} \begin{bmatrix} u \\ v \end{bmatrix} - \begin{bmatrix} \dot{x}_d \\ \dot{y}_d \end{bmatrix} \tag{14}$$

In addition, the velocity and yaw angular velocity tracking errors are defined as follows:

$$\begin{aligned} u_e &= u - \alpha_u \\ v_e &= v - \alpha_v \\ r_e &= r - \alpha_r \end{aligned} \tag{15}$$

where virtual controls α_u, α_v and α_r are designed as desired velocities and yaw angular velocity of the u, v and r, respectively.

According to equations of hovercraft dynamics (8) and (14), the derivatives of the tracking error of velocities and yaw angular velocity can be obtained as follows:

$$\begin{aligned} \dot{u}_e &= vr + \frac{F_{xD0}}{m_0} + f_u + \frac{\tau_u}{m_0} - \dot{\alpha}_u \\ \dot{v}_e &= -ur + \frac{F_{yD0}}{m_0} + f_v - \dot{\alpha}_v \\ \dot{r}_e &= \frac{M_{zD0}}{J_{z0}} + f_r + \frac{\tau_r}{J_{z0}} - \dot{\alpha}_r \end{aligned} \tag{16}$$

The problems solved in this paper can be formulated as follows:

Considering the hovercraft models (7) and (8) in existence of the model uncertainties and external disturbances, a finite-time adaptive PI sliding mode trajectory tracking controller is designed to generated surge force τ_u, desired yaw angular velocity α_r and yaw moment τ_r in order to guarantee velocity tracking errors u_e, v_e and yaw angular velocity tracking error r_e converge to zero in finite time. Then by the reasonable analysis and design of the desired velocities α_u and α_v, the position tracking errors x_e, y_e can converge to zero in finite time. At the same time, the drift angle is restricted in the control process, which ensures the safe navigation of the hovercraft.

III. CONTROLLER DESIGN

In this section, a trajectory tracking controller based on the adaptive finite-time PI sliding mode is designed for the underactuated hovercraft, and the uncertainty of the system is estimated and compensated by the finite-time observer. In order to ensure the navigation safety of the hovercraft, the drift angle β safety constraint auxiliary system of the hovercraft is designed to constrain the hovercraft's drift angle within the safety range.

A. DESIGN OF THE DESIRED VELOCITIES

The desired surge and sway velocities as virtual control laws of position errors are designed as follows:

$$\begin{bmatrix} \alpha_u \\ \alpha_v \end{bmatrix} = \begin{bmatrix} \cos\psi & \sin\psi \\ -\sin\psi/\cos\phi & \cos\psi/\cos\phi \end{bmatrix} \times \begin{bmatrix} \dot{x}_d - k_{x1}x_e - k_{x2}sign(x_e)|x_e|^{\frac{1}{2}} \\ \dot{y}_d - k_{y1}y_e - k_{y2}sign(y_e)|y_e|^{\frac{1}{2}} \end{bmatrix} \quad (17)$$

where k_{x1}, k_{x2}, k_{y1} and k_{y2} are positive design constants.

Assumption 6: The roll angle of the hovercraft satisfies inequality: $|\phi| < 90°$.

Remark 3: In the normal motion control process of hovercraft, ϕ is impossible to achieve $\pm 90°$ due to the effect of roll restoring moment. If the external environment disturbance breaks the balance relationship, the control task of this paper also loses its significance.

If the velocity errors u_e and v_e converge to zero in finite time, we have:

$$\begin{bmatrix} u \\ v \end{bmatrix} = \begin{bmatrix} \cos\psi & \sin\psi \\ -\sin\psi/\cos\phi & \cos\psi/\cos\phi \end{bmatrix} \times \begin{bmatrix} \dot{x}_d - k_{x1}x_e - k_{x2}sign(x_e)|x_e|^{\frac{1}{2}} \\ \dot{y}_d - k_{y1}y_e - k_{y2}sign(y_e)|y_e|^{\frac{1}{2}} \end{bmatrix} \quad (18)$$

By substituting (18) into (14), we can obtain the following equation:

$$\begin{aligned} \dot{x}_e + k_{x1}x_e + k_{x2}sign(x_e)|x_e|^{\frac{1}{2}} &= 0 \\ \dot{y}_e + k_{y1}y_e + k_{y2}sign(y_e)|y_e|^{\frac{1}{2}} &= 0 \end{aligned} \quad (19)$$

According to (19) we select Lyapunov function V_p about position errors:

$$V_p = \frac{1}{2}x_e^2 + \frac{1}{2}y_e^2 \quad (20)$$

According to Lemma 3, we can obtain the derivative of V_p:

$$\begin{aligned} \dot{V}_p &= x_e\dot{x}_e + y_e\dot{y}_e \\ &= -k_{x1}x_e^2 - k_{x2}|x_e|^{\frac{3}{2}} - k_{y1}y_e^2 - k_{y2}|y_e|^{\frac{3}{2}} \\ &\le -k_{m1}V_p - k_{m2}V_p^{\frac{3}{4}} \end{aligned} \quad (21)$$

where $k_{m1} = min\left(2k_{x1}, 2k_{y1}\right)$, $k_{m2} = min\left(2^{\frac{3}{4}}k_{x2}, 2^{\frac{3}{4}}k_{y2}\right)$.

According to lemma 4, when velocity tracking errors u_e and v_e converge to zero in finite time, the position tracking errors x_e, y_e converge to zero in finite time $t_p \le 4\ln\left(\left(k_{m1}V_p^{3/4}(0) + k_{m2}\right)/k_{m2}\right)/k_{m1}$ as well.

B. DESIGN OF THE SURGE FORCE

The surge force is designed to ensure velocity tracking error converges to zero in finite time. Since the dynamic model (8) contains model uncertainty and external disturbance, the following finite-time observer is designed to estimate it. Prior to the design the observer, the following extended state variables are defined:

$$\begin{cases} z_{u1} = u, & z_{u2} = f_u \\ z_{v1} = v, & z_{v2} = f_v \\ z_{r1} = r, & z_{r2} = f_r \end{cases} \quad (22)$$

Then we sequentially define $L_u = \dot{f}_u$, $L_v = \dot{f}_v$ and $L_r = \dot{f}_r$, according to Assumption 3 we easy know that L_u, L_v and L_r are bounded. Let's take the derivative of (22) with dynamic model (8) as follows:

$$\begin{cases} \dot{z}_{u1} = vr + \dfrac{F_{xD0}}{m_0} + \dfrac{\tau_u}{m_0} + z_{u2} \\ \dot{z}_{u2} = L_u \end{cases}$$
$$\begin{cases} \dot{z}_{v1} = -ur + \dfrac{F_{yD0}}{m_0} + z_{v2} \\ \dot{z}_{v2} = L_v \end{cases}$$
$$\begin{cases} \dot{z}_{r1} = \dfrac{M_{zD0}}{J_{z0}} + \dfrac{\tau_r}{J_{z0}} + z_{r2} \\ \dot{z}_{r2} = L_r \end{cases} \quad (23)$$

The finite-time observer is designed as follows:

$$\begin{cases} \dot{\hat{z}}_{u1} = vr + \dfrac{F_{xD0}}{m_0} + \dfrac{\tau_u}{m_0} + \hat{z}_{u2} + k_{u1}|e_{u1}|^{1/2}sign(e_{u1}) \\ \dot{\hat{z}}_{u2} = k_{u2}sign(e_{u1}) \end{cases}$$
$$\begin{cases} \dot{\hat{z}}_{v1} = -ur + \dfrac{F_{yD0}}{m_0} + \hat{z}_{v2} + k_{v1}|e_{v1}|^{1/2}sign(e_{v1}) \\ \dot{\hat{z}}_{v2} = k_{v2}sign(e_{v1}) \end{cases}$$
$$\begin{cases} \dot{\hat{z}}_{r1} = \dfrac{M_{zD0}}{J_{z0}} + \dfrac{\tau_r}{J_{z0}} + \hat{z}_{r2} + k_{r1}|e_{r1}|^{1/2}sign(e_{r1}) \\ \dot{\hat{z}}_{r2} = k_{r2}sign(e_{r1}) \end{cases} \quad (24)$$

where $e_{u1} = z_{u1} - \hat{z}_{u1}$, $e_{v1} = z_{v1} - \hat{z}_{v1}$ and $e_{r1} = z_{r1} - \hat{z}_{r1}$ are estimation errors of the observer. k_{u1}, k_{u2}, k_{v1}, k_{v2}, k_{r1} and k_{r2} are positive observer gains, according to (24) we can obtain the state equation of the observer errors as follows:

$$\begin{cases} \dot{e}_{u1} = -k_{u1}|e_{u1}|^{1/2}sign(e_{u1}) + e_{u2} \\ \dot{e}_{u2} = -k_{u2}sign(e_{u1}) + L_u \end{cases}$$
$$\begin{cases} \dot{e}_{v1} = -k_{v1}|e_{v1}|^{1/2}sign(e_{v1}) + e_{v2} \\ \dot{e}_{v2} = -k_{v2}sign(e_{v1}) + L_v \end{cases}$$
$$\begin{cases} \dot{e}_{r1} = -k_{r1}|e_{r1}|^{1/2}sign(e_{r1}) + e_{r2} \\ \dot{e}_{r2} = -k_{r2}sign(e_{r1}) + L_r \end{cases} \quad (25)$$

where $e_{u2} = z_{u2} - \hat{z}_{u2}$, $e_{v2} = z_{v2} - \hat{z}_{v2}$ and $e_{r2} = z_{r2} - \hat{z}_{r2}$.

According to lemma 2, the above observation errors system is finite-time stable. By selecting appropriate parameters k_{u1}, k_{u2}, k_{v1}, k_{v2}, k_{r1} and k_{r2} the observer errors can converge to equilibrium point $e_{u1} = 0$, $e_{u2} = 0$, $e_{v1} = 0$, $e_{v2} = 0$, $e_{r1} = 0$ and $e_{r2} = 0$ in finite time t_{f1}, that is, the following equation is true after time t_{f1}:

$$\begin{cases} \hat{z}_{u1} = u, & \hat{z}_{u2} = f_u \\ \hat{z}_{v1} = v, & \hat{z}_{v2} = f_v \\ \hat{z}_{r1} = r, & \hat{z}_{r2} = f_r \end{cases} \quad (26)$$

Next, the surge force τ_u is designed to make the surge velocity error converge to zero in finite time. Design the sliding surface s_1:

$$s_1 = u_e + \int_0^t k_1 sign\,(u_e)|u_e|^{\alpha_1} d\sigma \tag{27}$$

where parameters k_1 and α_1 are determined by the rules in the Lemma 1.

Based on (16), the derivative of s_1 is:

$$\begin{aligned}\dot{s}_1 &= \dot{u}_e + k_1 sign\,(u_e)\,|u_e|^{\alpha_1} \\ &= vr + \frac{F_{xD0}}{m_0} + f_u + \frac{\tau_u}{m_0} - \dot{\alpha}_u + k_1 sign\,(u_e)\,|u_e|^{\alpha_1}\end{aligned} \tag{28}$$

Consider the Lyapunov function V_1 as:

$$V_1 = \frac{1}{2}s_1^2 \tag{29}$$

By using (28), the derivative of V_1 yields:

$$\begin{aligned}\dot{V}_1 &= s_1\dot{s}_1 \\ &= s_1\left(vr + \frac{F_{xD0}}{m_0} + f_u + \frac{\tau_u}{m_0} - \dot{\alpha}_u + k_1 sign\,(u_e)\,|u_e|^{\alpha_1}\right)\end{aligned} \tag{30}$$

According to (30), the surge control law is designed as follows:

$$\begin{aligned}\tau_u = m_0\Big(&-vr - \frac{F_{xD0}}{m_0} - \hat{z}_{u2} - k_1 sign\,(u_e)\,|u_e|^{\alpha_1} + \dot{\alpha}_u \\ &-\eta_1 sign\,(s_1) - \eta_2 sign\,(s_1)\,|s_1|^{\frac{1}{2}} - k_{s1}s_1\Big)\end{aligned} \tag{31}$$

where $\eta_1 \geq \varepsilon_{u\max}$ is a very small design constant which can offset the estimation error of the finite-time observer. $\varepsilon_{u\max} > |e_{u2}|$, $\eta_2 > 0$ and $k_{s1} > 0$ are constants.

By substituting (31) into (30), we can get the derivative of V_1 as follows:

$$\begin{aligned}\dot{V}_1 &= s_1\left(f_u - \hat{z}_{u2} - \eta_1 sign\,(s_1) - \eta_2 sign\,(s_1)\,|s_1|^{\frac{1}{2}} - k_{s1}s_1\right) \\ &\leq -\eta_1\,|s_1| - \eta_2|s_1|^{\frac{3}{2}} - k_{s1}s_1^2 + |s_1|\,|e_{u2}| \\ &\leq -\eta_1\,|s_1| - \eta_2|s_1|^{\frac{3}{2}} - k_{s1}s_1^2 + |s_1|\,|\varepsilon_{u\max}| \\ &\leq -\eta_2|s_1|^{\frac{3}{2}} - k_{s1}s_1^2\end{aligned} \tag{32}$$

C. DESIGN OF THE DESIRED YAW ANGULAR VELOCITY

Next, the desired yaw angular velocity α_r is designed as a stability function to guarantee the sway velocity error converge to zero in a finite time. Design the sliding surface s_2:

$$s_2 = v_e + \int_0^t k_2 sign\,(v_e)|v_e|^{\alpha_2} d\sigma \tag{33}$$

where parameters k_2 and α_2 are selected via the rules in the Lemma 1.

Substituting (16) into (33), the derivative of s_2 is:

$$\begin{aligned}\dot{s}_2 &= \dot{v}_e + k_2 sign\,(v_e)\,|v_e|^{\alpha_2} \\ &= -ur + \frac{F_{yD0}}{m_0} + f_v - \dot{\alpha}_v + k_2 sign\,(v_e)\,|v_e|^{\alpha_2}\end{aligned} \tag{34}$$

Consider the Lyapunov function V_2 as:

$$V_2 = \frac{1}{2}s_2^2 \tag{35}$$

Using (34), the derivative of V_2 as follows:

$$\begin{aligned}\dot{V}_2 &= s_2\dot{s}_2 \\ &= s_2\left(-ur + \frac{F_{yD0}}{m_0} + f_v - \dot{\alpha}_v + k_2 sign\,(v_e)\,|v_e|^{\alpha_2}\right)\end{aligned} \tag{36}$$

According to (36), the desired yaw angular velocity α_r is designed as follows:

$$\begin{aligned}\alpha_r = \Big(&\frac{F_{yD0}}{m_0} + \hat{z}_{v2} - \dot{\alpha}_v + k_2 sign\,(v_e)\,|v_e|^{\alpha_2} \\ &+ \eta_3 sign\,(s_2) + \eta_4 sign\,(s_2)\,|s_2|^{\frac{1}{2}} + k_{s2}s_2\Big)\Big/u\end{aligned} \tag{37}$$

where $\eta_2 \geq \varepsilon_{v\max}$, $\varepsilon_{v\max} > |e_{v2}|$ is very small constant, $\eta_4 > 0$, $k_{s2} > 0$ are constants.

Remark 4: Hovercraft relies on air propeller to provide forward power. In normal motion control, the pitch angle is positive. Only in special cases, such as entering and leaving the mother ship, the negative pitch angle can be set. Therefore, in the motion control process of hovercraft we set surge speed $u > 0$.

Define the yaw angular velocity error variable $r_e = r - \alpha_r$, when r_e converge to zero in finite time the equation $r = \alpha_r$ holds. By substituting (37) into (36), we can obtain the derivative of V_2 as follows:

$$\begin{aligned}\dot{V}_2 &= s_2\left(-ur + \frac{F_{yD0}}{m_0} + f_v - \dot{\alpha}_v + k_2 sign\,(v_e)\,|v_e|^{\alpha_2}\right) \\ &= s_2\left(f_v - \hat{z}_{v2} - \eta_3 sign\,(s_2) - \eta_4 sign\,(s_2)\,|s_2|^{\frac{1}{2}} - k_{s2}s_2\right) \\ &\leq -\eta_3\,|s_2| + \varepsilon_{v\max}\,|s_2| - \eta_4|s_2|^{\frac{3}{2}} - k_{s2}s_2^2 \\ &\leq -\eta_4|s_2|^{\frac{3}{2}} - k_{s2}s_2^2\end{aligned} \tag{38}$$

D. DESIGN OF THE YAW MOMENT

Next, we design the yaw moment τ_r to stabilize yaw angular velocity error r_e, Firstly, the input of safety constraint auxiliary system of hovercraft drift angle β is defined as follows:

$$\Delta\beta = k_\beta\,(\beta_{\max} - \beta) \tag{39}$$

where k_β is positive coefficient, $\beta_{\max}$ can be determined by the following equation:

$$\beta_{\max} = sat(\beta, 2) = \begin{cases} 2 & \beta > 2 \\ \beta & -2 \leq \beta \leq 2 \\ -2 & \beta < -2 \end{cases} \tag{40}$$

Design safety constraint auxiliary system [28]:

$$\dot{\xi}_\beta = \begin{cases} -k_{\xi\beta 1}\xi_\beta - k_{\xi\beta 2} sign\left(\xi_\beta\right)\left|\xi_\beta\right|^{\frac{1}{2}} \\ \quad -\dfrac{\frac{1}{2}(k_{\xi\beta 3}\Delta\beta)^2}{\left|\xi_\beta\right|^2}\xi_\beta + k_{\xi\beta 3}\Delta\beta, & \left|\xi_\beta\right| \geq \varpi \\ 0, & \left|\xi_\beta\right| < \varpi \end{cases} \tag{41}$$

where $k_{\xi\beta 1} > 1$, $k_{\xi\beta 2} > 0$ and $k_{\xi\beta 3} > 0$ are parameters of the safety constraint auxiliary system, $\varpi > 0$ is very small constant.

In order to obtain yaw moment τ_r, design the sliding surface s_3:

$$s_3 = r_e + \int_0^t k_3 sign\,(r_e)|r_e|^{\alpha_3} d\sigma \tag{42}$$

where parameters k_3 and α_3 are determined via the rules in the Lemma 1.

Considering (16), the derivative of s_3 is:

$$\begin{aligned}\dot{s}_3 &= \dot{r}_e + k_3 sign\,(r_e)\,|r_e|^{\alpha_3} \\ &= \frac{M_{zD0}}{J_{z0}} + f_r + \frac{\tau_r}{J_{z0}} - \dot{\alpha}_r + k_3 sign\,(r_e)\,|r_e|^{\alpha_3}\end{aligned} \tag{43}$$

Select the Lyapunov function V_3 as:

$$V_3 = \frac{1}{2}s_3^2 + \frac{1}{2}\xi_\beta^2 \tag{44}$$

In the light of (43) and (41), the derivative of V_3 can determined as follows:

$$\begin{aligned}\dot{V}_3 &= s_3\dot{s}_3 + \xi_\beta\dot{\xi}_\beta \\ &= s_3\left(\frac{M_{zD0}}{J_{z0}} + f_r + \frac{\tau_r}{J_{z0}} - \dot{\alpha}_r + k_3 sign\,(r_e)\,|r_e|^{\alpha_3}\right) \\ &\quad - k_{\xi\beta 1}\xi_\beta^2 - k_{\xi\beta 2}\left|\xi_\beta\right|^{\frac{3}{2}} - \frac{1}{2}(k_{\xi\beta 3}\Delta\beta)^2 + k_{\xi\beta 3}\Delta\beta\xi_\beta\end{aligned} \tag{45}$$

According to (45), the yaw moment τ_r is designed as follows:

$$\begin{aligned}\tau_r = J_{z0}\Bigg(&-\frac{M_{zD0}}{J_{z0}} - \hat{z}_{r2} - k_3 sign\,(r_e)\,|r_e|^{\alpha_3} + \dot{\alpha}_r \\ &- \eta_5 sign\,(s_3) - \eta_6 sign\,(s_3)\,|s_3|^{\frac{1}{2}} - k_{s3}s_3 \\ &+ k_{\beta s3}\xi_\beta - \frac{k_{\beta s3}^2}{2}s_3\Bigg)\end{aligned} \tag{46}$$

where $\eta_5 \geq \varepsilon_{r\max}$, $\varepsilon_{r\max} > |e_{r2}|$ is very small constant, $\eta_6 > 0$ and $k_{s3} > 0$ are constants.

By substituting (46) into (45), the derivative of V_3 can be rewritten as follows:

$$\begin{aligned}\dot{V}_3 &= s_3\Bigg(f_r - \hat{z}_{r2} - \eta_5 sign\,(s_3) - \eta_6 sign\,(s_3)\,|s_3|^{\frac{1}{2}} \\ &\quad - k_{s3}s_3 + k_{\beta s3}\xi_\beta - \frac{k_{\beta s3}^2}{2}s_3\Bigg) - k_{\xi\beta 1}\xi_\beta^2 - k_{\xi\beta 2}\left|\xi_\beta\right|^{\frac{3}{2}} \\ &\quad - \frac{1}{2}(k_{\xi\beta 3}\Delta\beta)^2 + k_{\xi\beta 3}\Delta\beta\xi_\beta \\ &\leq -\eta_5\,|s_3| - \eta_6|s_3|^{\frac{3}{2}} - k_{s3}s_3^2 + |s_3|\,|e_{r2}| \\ &\quad - \left(k_{\xi\beta 1} - 1\right)\xi_\beta^2 - k_{\xi\beta 2}\left|\xi_\beta\right|^{\frac{3}{2}} \\ &\leq -\eta_5\,|s_3| - \eta_6|s_3|^{\frac{3}{2}} - k_{s3}s_3^2 + |s_3|\,|\varepsilon_{u\max}| \\ &\quad - \left(k_{\xi\beta 1} - 1\right)\xi_\beta^2 - k_{\xi\beta 2}\left|\xi_\beta\right|^{\frac{3}{2}} \\ &\leq -\eta_6|s_3|^{\frac{3}{2}} - k_{s3}s_3^2 - \left(k_{\xi\beta 1} - 1\right)\xi_\beta^2 - k_{\xi\beta 2}\left|\xi_\beta\right|^{\frac{3}{2}}\end{aligned} \tag{47}$$

E. STABILITY ANALYSIS

Theorem 1: Consider the hovercraft trajectory tracking nonlinear system (7) and (8) under unknown terms, suppose that Assumptions 1-6 are satisfied. The reasonable design of the desired surge and sway velocities and yaw angular velocity are calculated by (17) and (37), the finite-time PI sliding mode controllers are obtained by (31) and (46), the model uncertainties and external disturbances are estimated by the finite-time observer (25), and the safety constraint auxiliary system of hovercraft drift angle β is designed as (41), then all tracking errors can be ensured to converge to zero in finite time, the drift angle β can be restrained in real time and all closed-loop signals in the system are bounded.

Proof: Consider the following Lyapunov function V:

$$\begin{aligned}V &= V_1 + V_2 + V_3 \\ &= \frac{1}{2}s_1^2 + \frac{1}{2}s_2^2 + \frac{1}{2}s_3^2 + \frac{1}{2}\xi_\beta^2\end{aligned} \tag{48}$$

With the help of (32), (38) and (47), the time derivative of the (48) satisfies:

$$\begin{aligned}\dot{V} &= s_1\dot{s}_1 + s_2\dot{s}_2 + s_3\dot{s}_3 + \xi_\beta\dot{\xi}_\beta \\ &\leq -\eta_2|s_1|^{\frac{3}{2}} - k_{s1}s_1^2 - \eta_4|s_2|^{\frac{3}{2}} - k_{s2}s_2^2 - \eta_6|s_3|^{\frac{3}{2}} \\ &\quad - k_{s3}s_3^2 - \left(k_{\xi\beta 1} - 1\right)\xi_\beta^2 - k_{\xi\beta 2}\left|\xi_\beta\right|^{\frac{3}{2}}\end{aligned} \tag{49}$$

According to Lemma 3, we have:

$$\begin{aligned}\dot{V} &\leq -\eta_2|s_1|^{\frac{3}{2}} - k_{s1}s_1^2 - \eta_4|s_2|^{\frac{3}{2}} - k_{s2}s_2^2 - \eta_6|s_3|^{\frac{3}{2}} \\ &\quad - k_{s3}s_3^2 - \left(k_{\xi\beta 1} - 1\right)\xi_\beta^2 - k_{\xi\beta 2}\left|\xi_\beta\right|^{\frac{3}{2}} \\ &\leq -\lambda_1 V - 2^{\frac{3}{4}}\lambda_2 V^{\frac{3}{4}}\end{aligned} \tag{50}$$

where

$$\begin{aligned}\lambda_1 &= \min\left(2k_{s1}, 2k_{s2}, 2k_{s3}, 2\left(k_{\xi\beta 1} - 1\right)\right) \\ \lambda_2 &= \min\left(\eta_2, \eta_4, \eta_6, k_{\xi\beta 2}\right)\end{aligned} \tag{51}$$

Based on Lemma 4, the sliding surfaces s_1, s_2, s_3 and safety constraint auxiliary system ξ_β can converge to zero in finite time t_s:

$$t_s \leq \frac{1}{\lambda_1\left(1 - 3/4\right)}\ln\frac{\lambda_1 V^{\frac{3}{4}}(x(0)) + 2^{\frac{3}{4}}\lambda_2}{2^{\frac{3}{4}}\lambda_2} \tag{52}$$

Considering the drift angle β safety constraint auxiliary system and the safety constraint compensation term $k_{\beta s3}\xi_\beta$ in yaw moment τ_r, we can adjust the constraint coefficient k_β and the control gain $k_{\beta s3}$ to ensure drift angle is restrained in real time, after time t_s the ξ_β converges to zero, so drift angle β is restrained in safety range.

According to the above analysis, after sliding surfaces s_1, s_2, s_3 converge to zero in finite time t_s, we can obtain:

$$\begin{aligned}s_1 &= u_e + \int_0^t k_1 sign\,(u_e)|u_e|^{\alpha_1} d\sigma = 0 \\ s_2 &= v_e + \int_0^t k_2 sign\,(v_e)|v_e|^{\alpha_2} d\sigma = 0\end{aligned}$$

$$s_3 = r_e + \int_0^t k_3 sign\,(r_e)|r_e|^{\alpha_3} d\sigma = 0 \tag{53}$$

Then derivatives of sliding surfaces s_1, s_2, s_3 are:

$$\begin{aligned} \dot{u}_e + k_1 sign\,(u_e)\,|u_e|^{\alpha_1} &= 0 \\ \dot{v}_e + k_2 sign\,(v_e)\,|v_e|^{\alpha_2} &= 0 \\ \dot{r}_e + k_3 sign\,(r_e)\,|r_e|^{\alpha_3} &= 0 \end{aligned} \tag{54}$$

According to Lemma 1, the surge and sway velocity errors u_e, v_e and yaw angular velocity error r_e converge to zero in finite time t_f. Further, based on analysis in the section 3.1, after velocity tracking errors u_e, v_e converge to zero in finite time t_f, the position errors x_e, y_e can converge to zero in finite time $t_{ptal} \leq t_s + t_f + t_p$ as well. Considering Lemma 2, observation errors e_{u1}, e_{u2}, e_{v1}, e_{v2}, e_{r1} and e_{r2} converge to zero in finite time. Further, according to Assumption 4 and Assumption 6, the virtual control $\alpha_u, \alpha_v, \alpha_r$ and the roll angular velocity p are bounded.

This completes the proof.

Remark 5: Compared with the previous work [29], in which the controllers can only ensure that the sliding mode surfaces asymptotically converge to zero, thus tracking errors can converge to zero in finite time only after the sliding mode surfaces converge to zero. However, the controller designed in this paper can guarantee that the sliding surfaces converge to zero in finite time. And in the same time, the drift angle β is restricted in real time.

Remark 6: The special structure of the PI sliding mode manifolds in this paper can relax some assumptions in [6], such as the existence of the first derivative of the control input. Therefore, the proposed control strategy is simple and easy to implement in practice.

TABLE 1. Main parameters of hovercraft.

Parameter	Value	Unit	Parameter	Value	Unit
m_0	40000	kg	J_{z0}	1.8×10^6	$kg \cdot m^2$
J_{x0}	2.5×10^5	$kg \cdot m^2$	S_{PP}	45	m^2
S_{LP}	93	m^2	S_{HP}	260	m^2
Q	140.8	m^3/s	S_c	212	m^2
l_{sk}	65	m	B_c	8.9	m
h_m	2.4	m	l_c	23.6	m
h	1	m	H_{hov}	5.9	m
V_w	5	$knot$	β_w	45	deg

IV. SIMULATIONS

In this section, the experiments of the control system of the hovercraft trajectory tracking are executed in MATLAB R2014a on the computer. The comparison with conventional PID control is performed to verify effectiveness and robustness of the proposed control scheme. In simulations, the hovercraft's main parameters are shown in Table 1 [29].

The control parameters are set as: $k_{x1} = 0.01$, $k_{x2} = 0.15$, $k_{y1} = 0.04$, $k_{y2} = 0.12$, $k_1 = 0.5$, $\alpha_1 = 0.8$, $k_2 = 0.05$, $\alpha_2 = 0.1$, $k_3 = 0.001$, $\alpha_3 = 0.55$, $\eta_1 = 0.02$, $\eta_2 = 0.01$, $\eta_3 = 0.08$, $\eta_4 = 0.06$, $\eta_5 = 0.01$, $\eta_6 = 0.059$, $k_{s1} = 0.1$, $k_{s2} = 0.001$, $k_{s3} = 0.0008$, $k_{\beta s3} = 2$. The parameters of the auxiliary system are selected as: $k_{\xi\beta 1} = 1.1$, $k_{\xi\beta 2} = 0.1$, $k_{\xi\beta 3} = 0.01$, $k_\beta = 1.1$, $\varpi = 0.00001$. The parameters of the finite-time observers are designed as: $k_{u1} = 0.85$, $k_{u2} = 0.05$, $k_{v1} = 0.8$, $k_{v2} = 0.05$, $k_{r1} = 0.03$, $k_{r2} = 0.0003$.

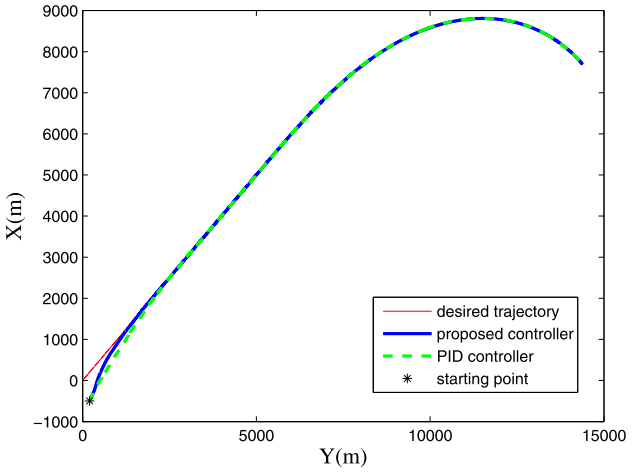

FIGURE 2. The actual and desired trajectory of hovercraft.

The initial values of the hovercraft model are set as: $x(0) = -500m$, $y(0) = 200m$, $\phi(0) = 0$, $\psi(0) = 30°$, $u(0) = 30knots$, $v(0) = 0$, $p(0) = 0$, $r(0) = 0$.

The parameters of the desired trajectory is generated by the virtual ship (11) are set as: $x_d(0) = 0$, $y_d(0) = 0$, $\psi_d(0) = 45°$, $u_{dset}(t) = 35knots$, $v_{dset}(t) = 0$ and

$$r_{dset}(t) = \begin{cases} 0 & t < t_c \\ sat(k_{rset}(t - t_c), r_c, -r_c) & t \geq t_c \end{cases} \tag{55}$$

where $t_c = 200s$, $r_c = 0.5°/s$,

$$sat(x, x\_max, x\_min) = \begin{cases} x\_max, x > x\_max \\ x, x\_min \leq x \leq x\_max \\ x\_min, x < x\_min \end{cases} \tag{56}$$

The model uncertainties and external disturbances are described by the following formula:

$$\begin{bmatrix} f_u \\ f_v \\ f_r \end{bmatrix} = \begin{bmatrix} \dfrac{2\sin(0.05t)}{m_0} & & \\ & \dfrac{0.2\cos(0.03t)}{m_0} & \\ & & \dfrac{\cos(0.02t)}{J_{z0}} \end{bmatrix} \begin{bmatrix} b_1 \\ b_2 \\ b_3 \end{bmatrix}. \tag{57}$$

where $b = \begin{bmatrix} b_1 & b_2 & b_3 \end{bmatrix}^T \in R^3$, $\dot{b} = -T^{-1}b + Aw_n$ is the first order Markov process, $w_n \in R^3$ is the vector of zero-mean Gaussian white noises, the other parameters of the first order Markov process are set as:

$$\begin{aligned} b(0) &= [2 \times 10^4, 2 \times 10^4, 2 \times 10^4]^T \\ T &= diag(10^3, 10^3, 10^3) \\ A &= diag(1 \times 10^4, 1 \times 10^4, 1 \times 10^4) \end{aligned} \tag{58}$$

The simulation results are shown in Fig.2, 3, 4, 5, 6, 7, 8, 9 and 10. Fig.2 shows the hovercraft followed the

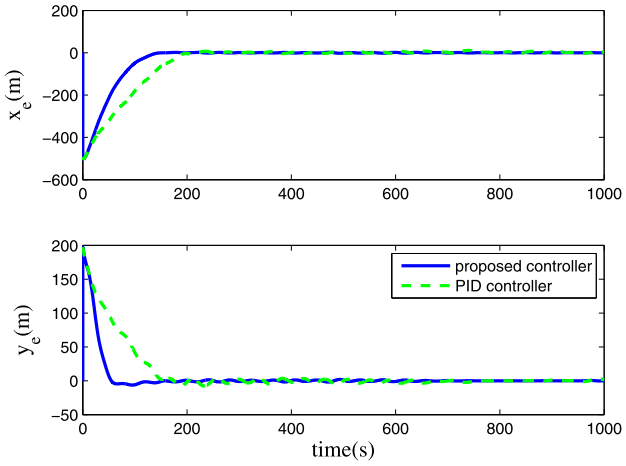

FIGURE 3. The position tracking errors of hovercraft.

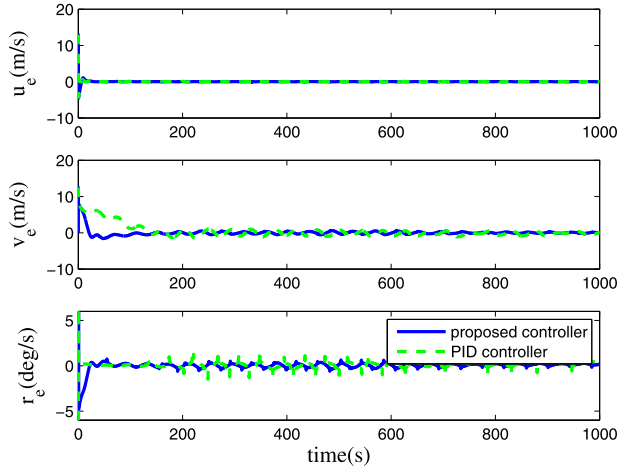

FIGURE 4. The velocity and rate of turning tracking errors of hovercraft.

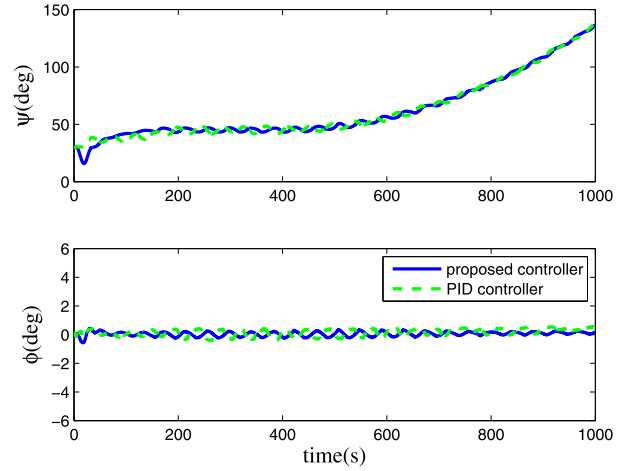

FIGURE 5. The yaw angular and roll angular of hovercraft.

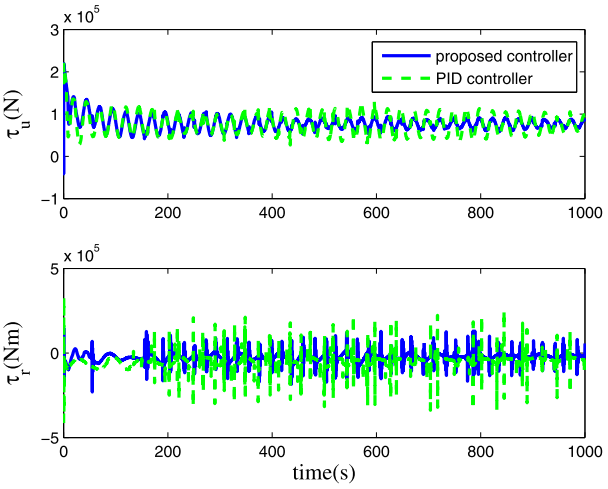

FIGURE 6. The surge control law and yaw control law of hovercraft.

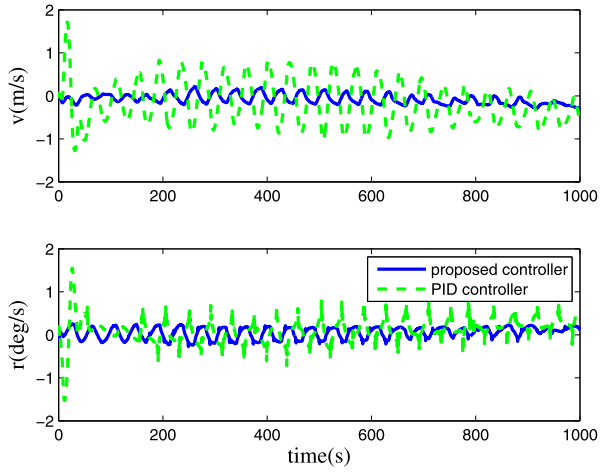

FIGURE 7. The sway velocity and rate of turning of hovercraft.

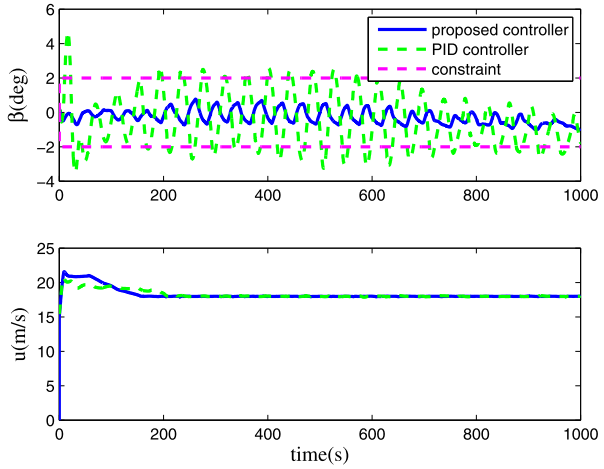

FIGURE 8. The drift angle and surge velocity of hovercraft.

desired trajectory in the presence of the model uncertainties and external disturbances. The desired trajectories are constructed by a straight line with a quasi-circle. Because this desired reference trajectories can represent somewhat realistic performance in the problem of trajectory tracking or path following. From Fig.3 and 4, it can be seen that the controllers designed in this paper is effective and ensure that no matter the tracking straight line or the quasi-circle the

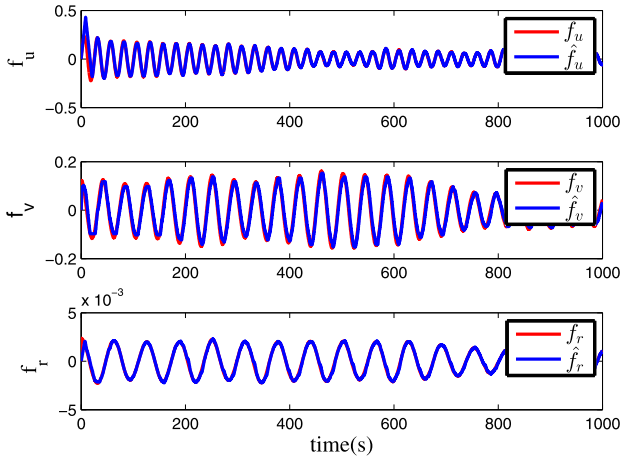

FIGURE 9. The model uncertainties and their estimated values of hovercraft.

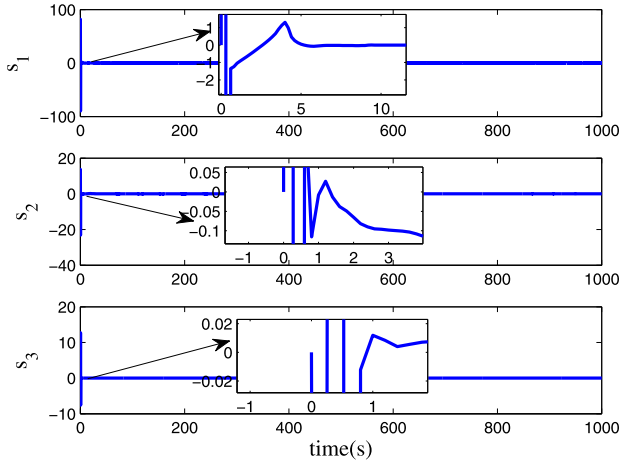

FIGURE 10. The evolution of the sliding mode manifold.

position tracking errors, velocities tracking errors and the yaw angular velocity tracking error can converge to a very small range near zero in finite time, and the proposed controllers have faster convergence speed and higher tracking accuracy than PID controller. The curves of the yaw angle, roll angle, sway velocity and yaw angular velocity vary with the time are shown in Fig.5 and 7. The control inputs under these two controllers are shown in Fig.6. It can be observed that the drift angle is restrained in real time under the proposed controllers in Fig.8. The uncertainties and the corresponding estimation values are shown in Fig.9. The curves of the sliding surface vary with time are presented in Fig.10. All shown simulation results are illustrated the superiority and robustness of the proposed method.

V. CONCLUSION

This paper presents a finite-time PI trajectory tracking control strategy for hovercraft with drift angle constraint. The control strategy enhances the robustness of the closed-loop system with model uncertainty and external disturbance. Based on the 4-DOF model, the desired velocities are designed according to the finite-time theory, and the desired yaw angular velocity is designed according to the finite-time PI sliding mode method. The velocity tracking errors and yaw angular velocity error are stabilized by the designed finite-time PI sliding mode controllers and all tracking errors can be guaranteed to converge to zero in finite time. The designed controllers can deal with the strong nonlinearity and uncertainty of the complex model of hovercraft by combining with the finite-time observer. The drift angle safety constraint auxiliary system can restrict the drift angle in real time as much as possible. The simulation results indicate the robustness and superiority of the proposed controller.

REFERENCES

[1] L. Yun and A. Bliault, *Theory and Design of Air Cushion Craft*. Oxford, U.K.: 2000, pp. 612–617.
[2] H. Fu, "Analysis and consideration on safety of all-lift hovercraft," *Ship Boat*, no. 6, pp. 1–3, Dec. 2008.
[3] M. Cohen, T. Miloh, and G. Zilman, "Wave resistance of a hovercraft moving in water with nonrigid bottom," *Ocean Eng.*, vol. 28, no. 11, pp. 1461–1478, 2001.
[4] V. M. Kozin and A. V. Pogorelova, "Variation in the wave resistance of an amphibian air-cushion vehicle moving over a broken-ice field," *J. Appl. Mech. Tech. Phys.*, vol. 48, no. 1, pp. 80–84, 2007.
[5] A. Behal, D. M. Dawson, W. E. Dixon, and Y. Fang, "Tracking and regulation control of an underactuated surface vessel with nonintegrable dynamics," *IEEE Trans. Autom. Control*, vol. 47, no. 3, pp. 495–500, Mar. 2002.
[6] J. Xu, M. Wang, and L. Qiao, "Dynamical sliding mode control for the trajectory tracking of underactuated unmanned underwater vehicles," *Ocean Eng.*, vol. 105, pp. 54–63, Sep. 2015.
[7] Z. Sun, G. Zhang, Y. Jian, and W. Zhang, "Research on the sliding mode control for underactuated surface vessels via parameter estimation," *Nonlinear Dyn.*, vol. 91, no. 2, pp. 1163–1175, 2018.
[8] T. Elmokadem, M. Zribi, and K. Youcef-Toumi, "Trajectory tracking sliding mode control of underactuated AUVs," *Nonlinear Dyn.*, vol. 84, no. 2, pp. 1079–1091, Apr. 2016.
[9] T. Elmokadem, M. Zribi, and K. Youcef-Toumi, "Terminal sliding mode control for the trajectory tracking of underactuated autonomous underwater vehicles," *Ocean Eng.*, vol. 129, pp. 613–625, Jan. 2016.
[10] W. He, Z. Yin, and C. Sun, "Adaptive neural network control of a marine vessel with constraints using the asymmetric barrier Lyapunov function," *IEEE Trans. Cybern.*, vol. 47, no. 7, pp. 1641–1651, Jul. 2017.
[11] B. S. Park, J.-W. Kwon, and H. Kim, "Neural network-based output feedback control for reference tracking of underactuated surface vessels," *Automatica*, vol. 77, pp. 353–359, Mar. 2017.
[12] G. Zhang, X. Zhang, and Y. Zheng, "Adaptive neural path-following control for underactuated ships in fields of marine practice," *Ocean Eng.*, vol. 104, pp. 558–567, Aug. 2015.
[13] L. Yu, G. Zhang, Z. Sun, and W. Zhang, "Robust adaptive formation control of underactuated autonomous surface vessels based on MLP and DOB," *Nonlinear Dyn.*, vol. 94, no. 1, pp. 503–519, 2018.
[14] K. D. Do, Z. P. Jiang, and J. Pan, "Robust adaptive path following of underactuated ships," in *Proc. IEEE Conf. Decis. Control*, Dec. 2004, pp. 3243–3248.
[15] K. D. Do, J. Pan, and Z. P. Jiang, "Robust adaptive control of underactuated ships on a linear course with comfort," *Ocean Eng.*, vol. 30, no. 17, pp. 2201–2225, 2003.
[16] Y. F. Peng, "Robust intelligent backstepping tracking control for uncertain non-linear chaotic systems using control technique," *Chaos Solitons Fractals*, vol. 41, no. 4, pp. 2081–2096, 2009.
[17] K. D. Do, Z. P. Jiang, and J. Pan, "Robust global stabilization of underactuated ships on a linear course: State and output feedback," *Int. J. Control*, vol. 76, no. 1, pp. 1–17, 2002.
[18] T. I. Fossen and A. Grovlen, "Nonlinear output feedback control of dynamically positioned ships using vectorial observer backstepping," *IEEE Trans. Control Syst. Technol.*, vol. 6, no. 1, pp. 121–128, Jan. 1998.
[19] G. Wen, S. S. Ge, C. L. P. Chen, F. Tu, and S. Wang, "Adaptive tracking control of surface vessel using optimized backstepping technique," *IEEE Trans. Cybern.*, vol. 49, no. 9, pp. 3420–3431, Sep. 2018.

[20] Z. Zhang and Y. Wu, "Further results on global stabilisation and tracking control for underactuated surface vessels with non-diagonal inertia and damping matrices," *Int. J. Control*, vol. 88, no. 9, pp. 1679–1692, 2015.
[21] H. Xin, J. Du, and J. Shi, "Adaptive fuzzy controller design for dynamic positioning system of vessels," *Appl. Ocean Res.*, vol. 53, pp. 46–53, Oct. 2015.
[22] X. Lin, J. Nie, Y. Jiao, K. Liang, and H. Li, "Adaptive fuzzy output feedback stabilization control for the underactuated surface vessel," *Appl. Ocean Res.*, vol. 74, pp. 40–48, May 2018.
[23] D. Qiu, Q. Wang, J. Yang, and J. She, "Adaptive fuzzy control for path tracking of underactuated ships based on dynamic equilibrium state theory," *Int. J. Comput. Intell. Syst.*, vol. 4, no. 6, pp. 1148–1157, 2011.
[24] C.-Z. Pan, X.-Z. Lai, S. X. Yang, and M. Wu, "A biologically inspired approach to tracking control of underactuated surface vessels subject to unknown dynamics," *Expert Syst. Appl.*, vol. 42, no. 4, pp. 2153–2161, Mar. 2015.
[25] D. D. Mu, G. F. Wang, and Y. S. Fan, "Tracking control of poddedpropulsion unmanned surface vehicle with unknown dynamics and disturbance under input saturation," *Int. J. Control, Autom. Syst.*, vol. 16, no. 4, pp. 1905–1915, 2018.
[26] Y. Zhang, S. Li, and X. Liu, "Adaptive near-optimal control of uncertain systems with application to underactuated surface vessels," *IEEE Trans. Control Syst. Technol.*, vol. 26, no. 4, pp. 1204–1218, Jul. 2017.
[27] G. Rigatos and S. Tzafestas, "Adaptive fuzzy control for the ship steering problem," *Mechatronics*, vol. 16, no. 8, pp. 479–489, Oct. 2006.
[28] M. Chen, S. S. Ge, and B. Ren, "Adaptive tracking control of uncertain MIMO nonlinear systems with input constraints," *Automatica*, vol. 47, no. 3, pp. 452–465, Mar. 2011.
[29] M. Fu, S. Gao, C. Wang, and M. Li, "Human-centered automatic tracking system for underactuated hovercraft based on adaptive chattering-free full-order terminal sliding mode control," *IEEE Access*, vol. 6, pp. 37883–37892, 2018.
[30] L.-X. Wang, *A Course in Fuzzy Systems and Control*. Upper Saddle River, NJ, USA: Prentice-Hall, 1996.
[31] Y. Feng, F. Han, and X. Yu, "Chattering free full-order sliding-mode control," *Automatica*, vol. 50, no. 4, pp. 1310–1314, 2014.
[32] J. A. Moreno and M. Osorio, "Strict Lyapunov functions for the super-twisting algorithm," *IEEE Trans. Autom. Control*, vol. 57, no. 4, pp. 1035–1040, Apr. 2012.
[33] A. Chalanga, S. Kamal, and B. Bandyopadhyay, "A new algorithm for continuous sliding mode control with implementation to industrial emulator setup," *IEEE/ASME Trans. Mechatronics*, vol. 20, no. 5, pp. 2194–2204, Oct. 2015.
[34] X. Jin, "Fault tolerant finite-time leader-follower formation control for autonomous surface vessels with LOS range and angle constraints," *Automatica*, vol. 68, pp. 228–236, Jun. 2016.
[35] O. Mofid and S. Mobayen, "Adaptive sliding mode control for finite-time stability of quad-rotor UAVs with parametric uncertainties," *ISA Trans.*, vol. 72, pp. 1–14, Jan. 2018.
[36] Z. Peng, D. Wang, Z. Chen, X. Hu, and W. Lan, "Adaptive dynamic surface control for formations of autonomous surface vehicles with uncertain dynamics," *IEEE Trans. Control Syst. Technol.*, vol. 21, no. 2, pp. 513–520, Mar. 2013.
[37] H. Sun, S. Li, and C. Sun, "Finite time integral sliding mode control of hypersonic vehicles," *Nonlinear Dyn.*, vol. 73, nos. 1–2, pp. 229–244, 2013.

MINGYU FU received the Ph.D. degree from the College of Automation, Harbin Engineering University, Harbin, China, in 2005. She is currently a Professor and the Ph.D. Supervisor with Harbin Engineering University. Her current research interests include vessel dynamic positioning control, automatic control of unmanned surface vehicle, and hovercraft motion control.

TAN ZHANG received the M.E. degree from the College of Automation, Harbin Engineering University, Harbin, China, in 2017, where he is currently pursuing the Ph.D. degree in control science and engineering with the College of Automation. His current research interests include robust adaptive control and motion control of the hovercraft.

FUGUANG DING received the M.E. degree from the College of Computer Science and Technology, Harbin Engineering University, Harbin, China, in 1996. He is currently a Professor and the M.E. Supervisor with the College of Automation, Harbin Engineering University. His main research interests include vessel dynamic positioning control, vessel intelligent control, and motion control of high-speed vessel.